

Closed-Form Expressions for the Current Densities on the Ground Planes of Asymmetric Stripline Structures

Christopher L. Holloway, *Senior Member, IEEE*, and Edward F. Kuester, *Fellow, IEEE*

Abstract—In this paper, closed-form expressions for the current density on the ground planes of an asymmetric stripline structure are derived. The derivation utilizes image theory in order to obtain a suitable quasi-static Green's function for this asymmetric geometry. For the special case of a symmetric stripline geometry and the limiting case of a microstrip line, it is demonstrated that the results obtained here reduce to previously derived results. As expected, it is illustrated that the current densities on the ground planes of an arbitrary asymmetric stripline are bounded by the current distribution of a symmetric stripline and that of a microstrip line. The validity of the analytical results is investigated by comparing to numerically obtained results. Finally, expressions are presented for the total ground-plane currents as fractions of the total current on the signal trace.

Index Terms—Asymmetric stripline, current density, ground plane, microstrip line, printed circuit board (PCB), signal integrity.

I. INTRODUCTION

STRIPLINE transmission structures are currently used in numerous high-speed electronic devices and products, ranging from signal traces on multilayer printed circuit boards (PCBs) to feeding networks in millimeter-wave and microwave integrated circuit (MIMIC) components. The current distribution on the ground planes of the stripline can be important for design considerations. Knowledge of these current distributions can aid in determining the amount of coupling between adjacent traces fabricated between two common ground planes, which is important in signal-integrity analysis [1]–[5]. These current distributions can also help determine how wide a truncated ground plane needs to be to ensure that edge effects are minimal.

The two-dimensional (2-D) asymmetric stripline geometry of interest in this paper is illustrated in Fig. 1. The signal trace (the center conductor) is infinitely long in the z direction and is centered about the origin (i.e., $x = y = 0$). The signal trace is assumed to be infinitely thin with a width w . The lower ground plane is located at the $y = -h_1$ plane, and the upper ground plane is located at $y = h_2$, giving a total plate separation of $l = h_1 + h_2$. Both ground planes and the signal trace are assumed to be perfect electric conductors (PECs).

Numerical techniques such as the finite element method (FEM) or integral equation method of moments (MOM) can

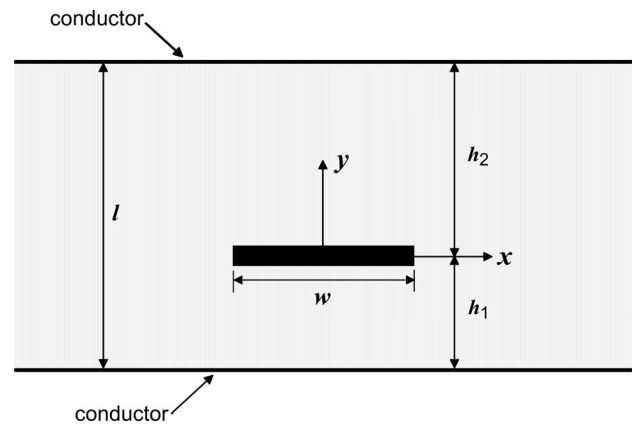


Fig. 1. Asymmetric stripline geometry.

be used to obtain the current distributions of the two ground planes for an asymmetric stripline structure. These techniques are very accurate; however, they can be computationally intensive and, hence, do not lend themselves to simple design procedures. Closed-form expressions for the current density on the two ground planes can be derived from an integration of the current on the signal trace with a suitable Green's function for an asymmetric geometry. The required Green's function is obtained from image theory, which requires summing the infinite number of images produced by the two ground planes. This paper presents such an approach. For a symmetric stripline geometry, where $h_1 = h_2$, the current density on the ground plane can be obtained from a spectral-domain approach; see [6] for details. The results in this paper reduce to the results of [6] when $h_1 = h_2$. If we allow $h_2 \rightarrow \infty$, the stripline geometry becomes a microstrip line. The current density for the ground plane of a microstrip line is given in [7]. The results here also reduce to those presented in [7] when we allow $h_2 \rightarrow \infty$.

The paper is organized as follows: Section II presents the Green's function approach and illustrates how it is used to obtain the current distributions. Section III presents the calculation of the magnetic field H for a line source between two parallel planes. In Section IV, these magnetic field expressions are used to obtain the needed Green's function, and hence, the desired closed-form current densities on the ground planes are obtained. Section V investigates important special cases of these closed-form expressions. The validity of these expressions are demonstrated in Section VI, where comparisons are made to numerical results for the ground plane current obtained from

Manuscript received May 9, 2006; revised October 16, 2006.

C. L. Holloway is with the Electromagnetics Division, Boulder Laboratories, National Institute of Standards and Technology, U.S. Department of Commerce, Boulder, CO 80305 USA (e-mail: holloway@boulder.nist.gov).

E. F. Kuester is with the Department of Electrical and Computer Engineering, University of Colorado, Boulder, CO 80309 USA.

Digital Object Identifier 10.1109/TEMC.2006.890219

FEM calculations. In Section VII, expressions are presented for the total current on each ground plane as a fraction of the total current on the signal trace for arbitrary h_2/h_1 . Section VIII summarizes the results presented here.

II. FORMULATION

For good conductors, the magnetic fields on the surface of the ground planes is only slightly perturbed from that at a PEC. Therefore, since we are interested in only the currents on the ground planes (not the currents inside the conductors), we have assumed PECs in this paper.

We further assume that the fields can be computed quasistatically. In general, all three vector components of currents and fields may exist. However, in planar circuits, the longitudinal component (J_z) of the current is usually the dominant one. Schumacher [12] shows that up to 12 GHz, the ratio of the transverse- to longitudinal-current components on striplines of typical dimensions is less than 0.1, and Kobayashi [11] shows that up to 20 GHz, this ratio is less than 0.15. Thus, as discussed by Kobayashi, little generality is lost by assuming quasi-TEM conditions, which allows the fields to be calculated from a 2-D quasi-static analysis of the stripline.

From the boundary conditions for Maxwell's equations on perfect conductors, it is well known that if the H fields for a stripline are known, then the current density on the two ground planes can be determined. For the upper ground plane, we have

$$J_{\text{upper}}(x) = \bar{a}_n \times \bar{H}(x, y = h_2) = H_x(x, y = h_2) \quad (1)$$

and for the lower ground plane, we have

$$J_{\text{lower}}(x) = \bar{a}_n \times \bar{H}(x, y = -h_1) = -H_x(x, y = -h_1). \quad (2)$$

The H fields on the surface of the ground planes can be obtained from a quasi-static Green's function approach. In this approach, the Green's function for a line source between two parallel plates is integrated over the signal trace of the actual stripline geometry i.e.,

$$H_x(x, y) = \int_{-w/2}^{w/2} J_{\text{trace}}(x') G(x - x', y) dx'. \quad (3)$$

In this analysis, it is assumed that the current density of the signal trace is approximated by a constant distribution

$$J_{\text{trace}}(x') = \frac{I}{w}. \quad (4)$$

With this assumed trace-current density, the H_x fields on the two ground planes can be expressed as

$$H_x(x, y = h_2) = \frac{I}{w} \int_{-w/2}^{w/2} G(x - x', y = h_2, y' = 0) dx' \quad (5)$$

for the upper conductor, and

$$H_x(x, y = -h_1) = \frac{I}{w} \int_{-w/2}^{w/2} G(x - x', y = -h_1, y' = 0) dx'. \quad (6)$$

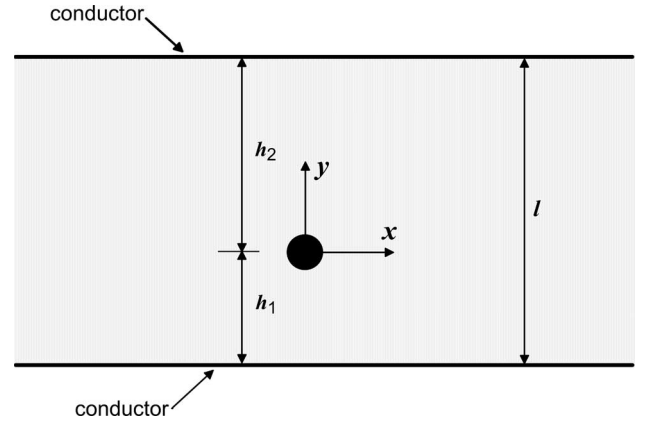


Fig. 2. Asymmetric line source located between two PEC plates.

for the lower conductor. The Green's function needed is essentially the H_x field for an infinite line source between two PEC parallel plates.

A word is in order about the assumed constant current distribution on the trace conductor and its consequences for the ground plane current. In reality, the exact current density at the edges of the trace must be singular and would be better approximated by a distribution, which possesses this behavior, such as the Maxwell or Kobayashi distribution [8]–[11]. In this paper, we show that for $w/h_1 < 0.5$, the current distribution on the ground planes resulting from assuming a constant trace-current distribution is indistinguishable from numerically computed results. For larger values of w/h_1 , some error in the ground plane current density directly under the trace occurs, but good correlation is obtained for the ground plane current from the edges of the trace to large values of $|x|/w$. Therefore, for practical geometries and applications, no generality is lost by assuming a constant current on the trace conductor.

III. H -FIELD OF A LINE SOURCE BETWEEN TWO PARALLEL PLATES

In this section, the H -field of a line source between two ground planes is obtained. The geometry of interest is shown in Fig. 2. It consists of an infinite line source lying along the z -axis and centered at the origin (i.e., $x' = y' = 0$). The lower ground plane is located at the $y = -h_1$ plane, and the upper ground plane is located at $y = h_2$. The total plate separation is $l = h_1 + h_2$. Both ground planes are assumed to be PECs.

The H -fields can be obtained from the z -component of the magnetic vector potential A [13]:

$$\begin{aligned} H_x &= \frac{1}{\mu_0} \frac{\partial}{\partial y} A_z \\ H_y &= -\frac{1}{\mu_0} \frac{\partial}{\partial x} A_z. \end{aligned} \quad (7)$$

The vector potential A_z for the geometry in Fig. 2 can be derived with the aid of image theory, wherein the ground planes in Fig. 2 are removed, and an infinite number of image sources are added; see Fig. 3. Note the alternating signs of the image currents.

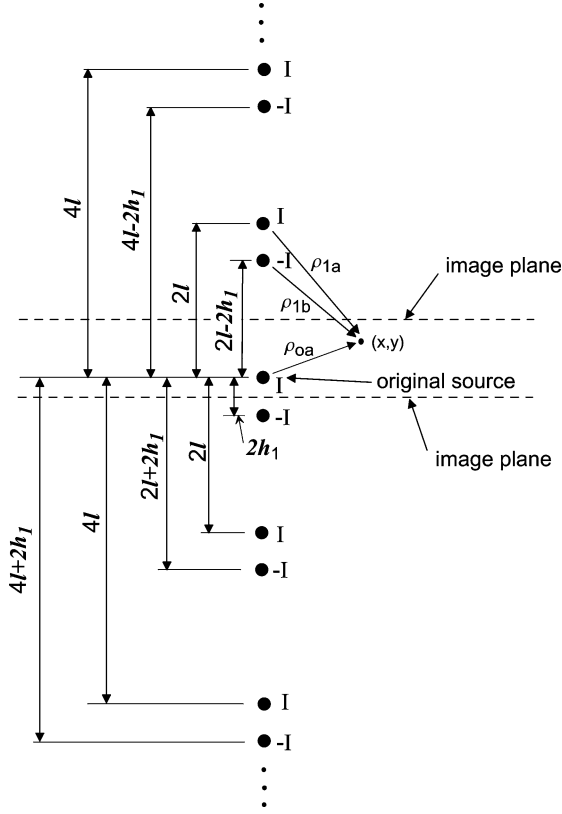


Fig. 3. Image-theory representation of an asymmetrically located line source between two PEC plates.

The vector potential for this infinite array of line sources is (see [13] and [14])

$$A_z = -\frac{\mu_0 I}{2\pi} \sum_{n=-\infty}^{\infty} \ln \frac{\rho_{na}}{\rho_{nb}} \quad (8)$$

where ρ_{na} and ρ_{nb} are the distances from each line source (the original source or one of the image sources) to an observation point (x, y) ; see Fig. 3. These distances are given by

$$\rho_{na} = \sqrt{x^2 + (y - 2nl)^2} \quad (9)$$

and

$$\rho_{nb} = \sqrt{x^2 + (y + 2h_1 - 2nl)^2} \quad (10)$$

where $l = h_1 + h_2$. Then, (8) can be expressed as

$$A_z = -\frac{\mu_0 I}{4\pi} \ln \left[\prod_{n=-\infty}^{\infty} \left(\frac{x^2 + (y - 2nl)^2}{x^2 + (y + 2h_1 - 2nl)^2} \right) \right]. \quad (11)$$

In earlier work, Hague [14] determined the magnetic field of a line source between two perfect iron regions (i.e., $\mu = \infty$) in a similar infinite product form. We will utilize his basic idea here. However, we modify Hague's approach by avoiding the appearance of divergent products that are found in [14].

The infinite product in (11) can be expressed as

$$\prod_{n=-\infty}^{\infty} \left(\frac{x^2 + (y - 2nl)^2}{x^2 + (y + 2h_1 - 2nl)^2} \right) = \prod_{n=-\infty}^{\infty} \left[\frac{1 + \left(\frac{x}{y - 2nl} \right)^2}{1 + \left(\frac{x}{y + 2h_1 - 2nl} \right)^2} \right] \times \prod_{n=-\infty}^{\infty} \left(\frac{y - 2nl}{y + 2h_1 - 2nl} \right)^2. \quad (12)$$

The first product on the right-hand side of (12) can be transformed as follows:

$$\prod_{n=-\infty}^{\infty} \left[\frac{1 + \left(\frac{x}{y - 2nl} \right)^2}{1 + \left(\frac{x}{y + 2h_1 - 2nl} \right)^2} \right] = \prod_{n=-\infty}^{\infty} \left[\frac{1 + \left(\frac{\pi x/l}{\pi y/l - 2\pi n} \right)^2}{1 + \left(\frac{\pi x/l}{\pi(y + 2h_1)/l - 2\pi n} \right)^2} \right] \\ = \frac{\cosh\left(\frac{\pi x}{l}\right) - \cos\left(\frac{\pi y}{l}\right)}{1 - \cos\left(\frac{\pi y}{l}\right)} \frac{1 - \cos\left(\frac{\pi(y + 2h_1)}{l}\right)}{\cosh\left(\frac{\pi x}{l}\right) - \cos\left(\frac{\pi(y + 2h_1)}{l}\right)} \quad (13)$$

where we have used formula given in [15, eq. (1.438)] (see also [14] and [16]–[18]). The second product on the right-hand side of (12) can be similarly transformed as

$$\prod_{n=-\infty}^{\infty} \left(\frac{y - 2nl}{y + 2h_1 - 2nl} \right)^2 = \prod_{n=-\infty}^{\infty} \left(\frac{n - y/2l}{n - (y + 2h_1)/2l} \right)^2 \\ = \left(\frac{y}{y + 2h_1} \right)^2 \prod_{n=1}^{\infty} \left[\frac{1 - \left(\frac{y}{2nl} \right)^2}{1 - \left(\frac{y + 2h_1}{2nl} \right)^2} \right]^2 \\ = \frac{\sin^2\left(\frac{\pi y}{2l}\right)}{\sin^2\left(\frac{\pi(y + 2h_1)}{2l}\right)} \quad (14)$$

where we have used formula given in [15, eq. (1.431.1)] (again, see also [14] and [16]–[18]). Combining (13) and (14) in (12) and using a trigonometric identity, (11) for the vector potential can be reduced to

$$A_z = -\frac{\mu_0 I}{4\pi} \ln \left[\frac{\cosh\left(\frac{\pi x}{l}\right) - \cos\left(\frac{\pi y}{l}\right)}{\cosh\left(\frac{\pi x}{l}\right) - \cos\left(\frac{\pi(y + 2h_1)}{l}\right)} \right]. \quad (15)$$

From (7), we obtain the H -fields by elementary differentiation

$$H_x = -\frac{I}{4l} \left[\frac{\sin\left(\frac{\pi y}{l}\right)}{\cosh\left(\frac{\pi x}{l}\right) - \cos\left(\frac{\pi y}{l}\right)} - \frac{\sin\left(\frac{\pi(y + 2h_1)}{l}\right)}{\cosh\left(\frac{\pi x}{l}\right) - \cos\left(\frac{\pi(y + 2h_1)}{l}\right)} \right] \quad (16)$$

and

$$H_y = \frac{I}{4l} \left[\frac{\sinh\left(\frac{\pi y}{l}\right)}{\cosh\left(\frac{\pi x}{l}\right) - \cos\left(\frac{\pi y}{l}\right)} - \frac{\sinh\left(\frac{\pi(y+2h_1)}{l}\right)}{\cosh\left(\frac{\pi x}{l}\right) - \cos\left(\frac{\pi(y+2h_1)}{l}\right)} \right]. \quad (17)$$

Finally, H_x on the upper ground plane is found to be

$$H_x(x)|_{y=h_2} = -\frac{I}{2l} \left[\frac{\sin\left(\frac{\pi h_2}{h_1+h_2}\right)}{\cosh\left(\frac{\pi x}{h_1+h_2}\right) - \cos\left(\frac{\pi h_2}{h_1+h_2}\right)} \right] \quad (18)$$

and on the lower ground plane is found to be

$$H_x(x)|_{y=-h_1} = \frac{I}{2l} \left[\frac{\sin\left(\frac{\pi h_1}{h_1+h_2}\right)}{\cosh\left(\frac{\pi x}{h_1+h_2}\right) - \cos\left(\frac{\pi h_1}{h_1+h_2}\right)} \right]. \quad (19)$$

IV. GROUND PLANE CURRENT DISTRIBUTIONS

From the results in (18) and (19), it is easily deduced that the Green's functions needed in (5) and (6) are given by

$$G(x-x', y=h_2) = -\frac{1}{2l} \left[\frac{\sin\left(\frac{\pi h_2}{h_1+h_2}\right)}{\cosh\left(\frac{\pi(x-x')}{h_1+h_2}\right) - \cos\left(\frac{\pi h_2}{h_1+h_2}\right)} \right] \quad (20)$$

and

$$G(x-x', y=-h_1) = \frac{1}{2l} \left[\frac{\sin\left(\frac{\pi h_1}{h_1+h_2}\right)}{\cosh\left(\frac{\pi(x-x')}{h_1+h_2}\right) - \cos\left(\frac{\pi h_1}{h_1+h_2}\right)} \right]. \quad (21)$$

These Green's functions are substituted into the expressions in (5) and (6) to obtain the H -fields. In order to determine the H -fields (and, in turn, the current densities) on the ground plane of an asymmetric stripline, the indefinite integral

$$\int \frac{\sin a \, dz}{\cosh z - \cos a} = 2 \tan^{-1} \left[\frac{e^z - \cos a}{\sin a} \right] \quad (22)$$

is needed.

Substituting the Green's functions from (20) and (21) into (5) and (6), and using (22), the current density on the upper ground plane is found to be

$$J_{\text{upper}}(x) = \frac{I}{\pi w} \left[\tan^{-1} \left(\frac{e^{\frac{\pi(x-w/2)}{l}} - \cos\left(\frac{\pi h_2}{l}\right)}{\sin\left(\frac{\pi h_2}{l}\right)} \right) - \tan^{-1} \left(\frac{e^{\frac{\pi(x+w/2)}{l}} - \cos\left(\frac{\pi h_2}{l}\right)}{\sin\left(\frac{\pi h_2}{l}\right)} \right) \right] \quad (23)$$

and that on the lower ground plane is

$$J_{\text{lower}}(x) = \frac{I}{\pi w} \left[\tan^{-1} \left(\frac{e^{\frac{\pi(x-w/2)}{l}} - \cos\left(\frac{\pi h_1}{l}\right)}{\sin\left(\frac{\pi h_1}{l}\right)} \right) - \tan^{-1} \left(\frac{e^{\frac{\pi(x+w/2)}{l}} - \cos\left(\frac{\pi h_1}{l}\right)}{\sin\left(\frac{\pi h_1}{l}\right)} \right) \right]. \quad (24)$$

V. SPECIAL CASES

In this section, three special cases are examined: 1) a symmetric stripline where $h_1 = h_2$; 2) a microstrip line where $h_2 \rightarrow \infty$; and 3) an asymmetric stripline where $h_2 = 2h_1$. The first two cases are used as a means of validating the expressions for ground plane current density against previously obtained results, while the third case is a particular geometry that occurs often in multi-layer PCB layouts.

A. Symmetric Stripline ($h_1 = h_2$)

For a symmetric stripline geometry ($h_1 = h_2$), (23) and (24) reduce to the same expression. By substituting $h_2 = h_1$ into these expressions, the current density on both ground planes reduces to

$$J(x) = \frac{I}{\pi w} \left[\tan^{-1} \left(e^{\frac{\pi(x-w/2)}{2h_1}} \right) - \tan^{-1} \left(e^{\frac{\pi(x+w/2)}{2h_1}} \right) \right]. \quad (25)$$

This is the same result obtained in [6], which was derived from a spectral-domain approach. A different, empirically fit expression for this case had been given earlier by Zehentner [19], but it is valid only over a limited range of parameters.

As an additional validation, this expression can be integrated over the whole of either ground plane; such an integral gives $\int_{-\infty}^{\infty} J(x) dx = -I/2$. For a symmetric stripline, the current is equally divided between both ground planes; thus, the sum of the currents on both planes is $-I$.

B. Microstrip Line ($h_2 \rightarrow \infty$)

For a microstrip line, the upper ground is absent. This case can be obtained by taking the limit of the expressions given in (23) and (24) as $h_2 \rightarrow \infty$ (although care must be exercised). We examine (24) for the current density on the lower ground plane. It can be shown that

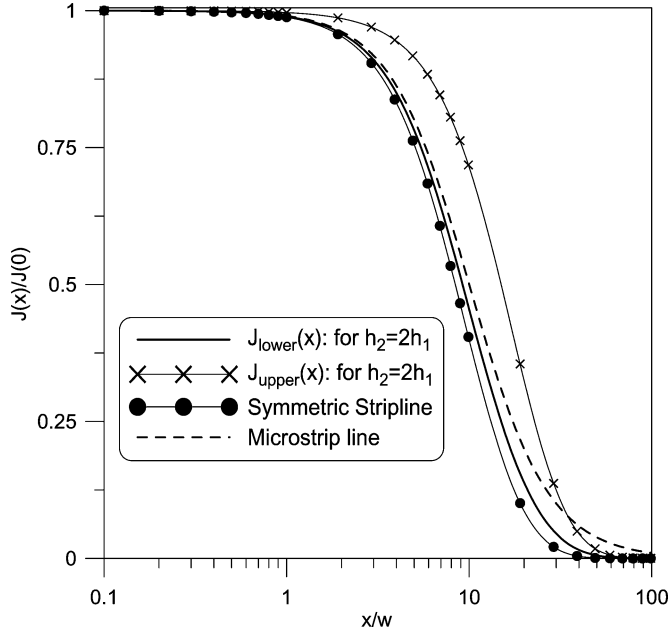
$$\lim_{u \rightarrow \infty} \frac{e^{a/u} - \cos(b/u)}{\sin(b/u)} = \frac{a}{b}. \quad (26)$$

Thus, the argument in the first term of (24) reduces to

$$\lim_{h_2 \rightarrow \infty} \frac{e^{\frac{\pi(x-w/2)}{l}} - \cos\left(\frac{\pi h_1}{l}\right)}{\sin\left(\frac{\pi h_1}{l}\right)} = \frac{2x-w}{2h_1} \quad (27)$$

with a similar result for the argument in the second term. Therefore, as $h_2 \rightarrow \infty$, the current density on the lower ground plane reduces to

$$J_{\text{lower}}(x)|_{h_2 \rightarrow \infty} = \frac{I}{\pi w} \left[\tan^{-1} \left(\frac{2x-w}{2h_1} \right) - \tan^{-1} \left(\frac{2x+w}{2h_1} \right) \right]. \quad (28)$$


 Fig. 4. Normalized current densities for $w/h_1 = 0.1$.

This is the same result obtained in [7] directly from a Green's function approach for the case of only one ground plane. Holloway and Kuester [7] compare this expression to both experimental and numerical results, and excellent agreement was found. Similarly, one can show that

$$J_{\text{upper}}(x)|_{h_2 \rightarrow \infty} \rightarrow 0. \quad (29)$$

As an additional validation, these two expressions can be integrated over their respective ground planes; the upper ground plane current is obviously zero, while $\int_{-\infty}^{\infty} J_{\text{lower}}(x) dx = -I$.

C. Asymmetric Stripline With $h_2 = 2h_1$

This particular configuration occurs for some multilayer PCBs. If we set $h_2 = 2h_1$ in (23) and (24), the following is obtained for the currents on the upper and lower ground planes, respectively:

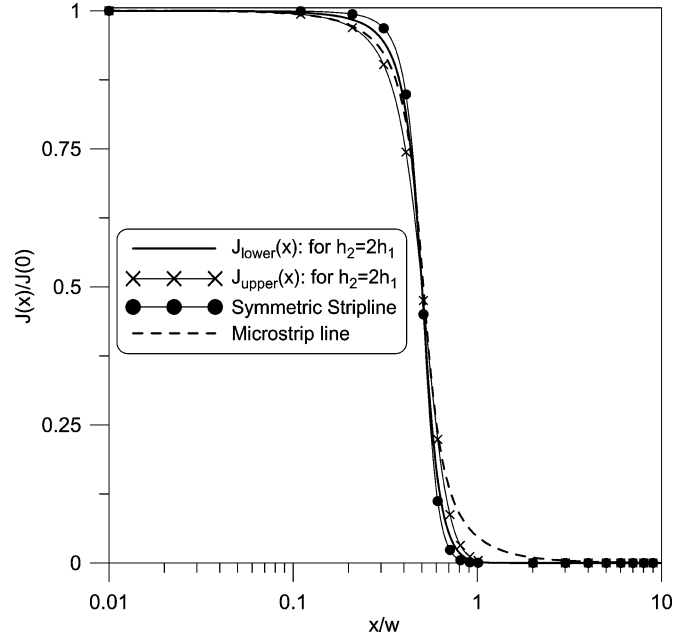
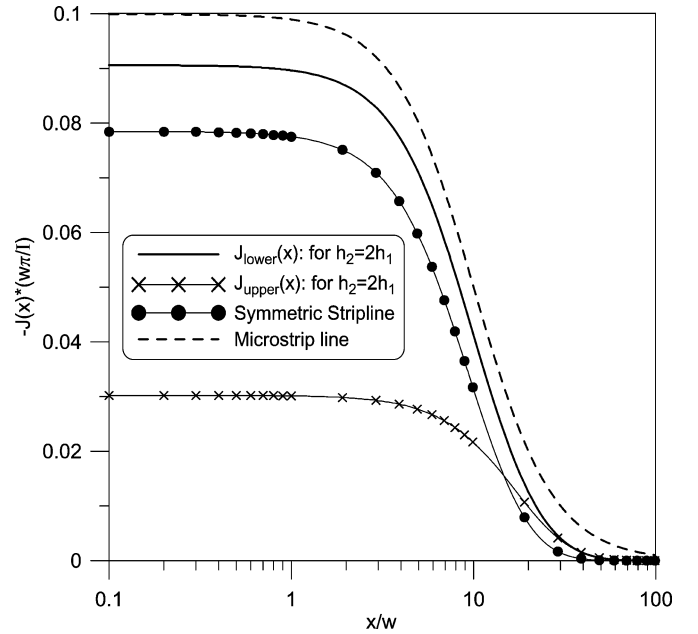
$$J_{\text{upper}}(x) = \frac{I}{\pi w} \left[\tan^{-1} \left(1.1547 e^{\frac{\pi(x-w/2)}{3h_1}} + 0.57735 \right) - \tan^{-1} \left(1.1547 e^{\frac{\pi(x+w/2)}{3h_1}} + 0.57735 \right) \right] \quad (30)$$

and

$$J_{\text{lower}}(x) = \frac{I}{\pi w} \left[\tan^{-1} \left(1.1547 e^{\frac{\pi(x-w/2)}{3h_1}} - 0.57735 \right) - \tan^{-1} \left(1.1547 e^{\frac{\pi(x+w/2)}{3h_1}} - 0.57735 \right) \right]. \quad (31)$$

The sum of the integrals of both these expressions over their respective ground planes equals $-I$.

These two expressions are plotted in Figs. 4–7 for various values of x/w and w/h_1 . Fig. 4 and 5 show results for the current densities normalized to $J(0)$ for $w/h_1 = 0.1$ and $w/h_1 = 10$, respectively. As a comparison, the results for a symmetric stripline and microstrip line are also shown in these


 Fig. 5. Normalized current densities for $w/h_1 = 10$.

 Fig. 6. Current densities of the different geometries for $w/h_1 = 0.10$.

figures. These normalized results illustrate how tightly confined under the signal trace the ground plane current is distributed. As expected, the results show that the current is more confined under the signal trace for the current on the lower ground plane than the current on the upper ground plane. This is expected, for when the signal trace becomes closer to a ground plane, more current is forced under the trace. This is also observed for a microstrip line; see [7]. Fig. 6 and 7 show results for the non-normalized current densities for $w/h_1 = 0.1$ and $w/h_1 = 10$, respectively. These results illustrate the relative magnitudes for the different geometries.

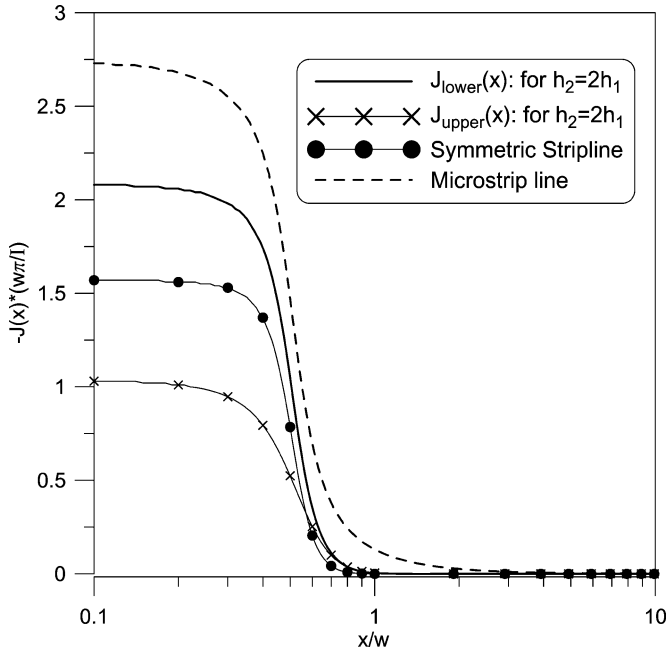


Fig. 7. Current densities of the different geometries for $w/h_1 = 10$.

VI. VALIDITY OF ANALYTICAL EXPRESSIONS: COMPARISON TO NUMERICAL CALCULATIONS

In order to validate the analytical expressions for the current density on the ground planes, we make comparisons to a full-numerical model of the stripline geometry. For this numerical comparison, the FEM technique was used [20]. In the numerical model, the ground planes were given widths of $10w$. Fig. 8 shows the analytical and numerical results for the current density on the lower ground plane for $w/h_1 = 0.5$ and $w/h_1 = 1.0$. Both these results are for $h_2 = 2h_1$. In this comparison, we see excellent correlation between the analytical and numerical results for $w/h_1 = 0.5$. For $w/h_1 = 1.0$, we see some deviation for points directly under the trace (i.e., $x/w < 0.5$). However, we see that the analytical results do an excellent job of representing the current beyond the edge of the trace (i.e., $x/w > 0.5$), even for the relatively large value of $w/h_1 = 1.0$. This is emphasized in Fig. 9, where we have replotted the results in Fig. 8 on a log scale. Excellent agreement to numerical results for the current on the upper ground plane was also obtained, and a comparison is shown in Fig. 10. Similar conclusions for the case of microstrip with even larger values of w/h_1 were reached in [7].

The deviation of the current density in the small region directly under the trace for large values of w/h_1 is due to the assumed constant current distribution on the trace, which was used in obtaining the analytical expressions. These results show that the effect of the current singularity at the edges of the trace shows up only for large w/h_1 . More importantly, the error is significant only for points directly under the trace, but once away from the trace, the ground plane current density obtained using a constant trace current does an excellent job of predicting the correct distribution. In fact, in many applications (e.g., for signal integrity considerations and coupling issues), we are only inter-

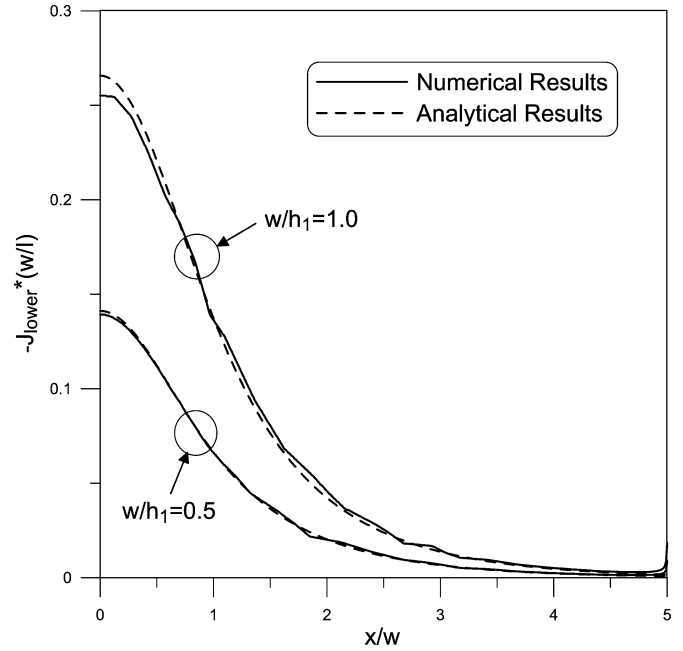


Fig. 8. Comparison of analytical and numerical results for the current on the lower ground plane for $h_2 = 2h_1$.

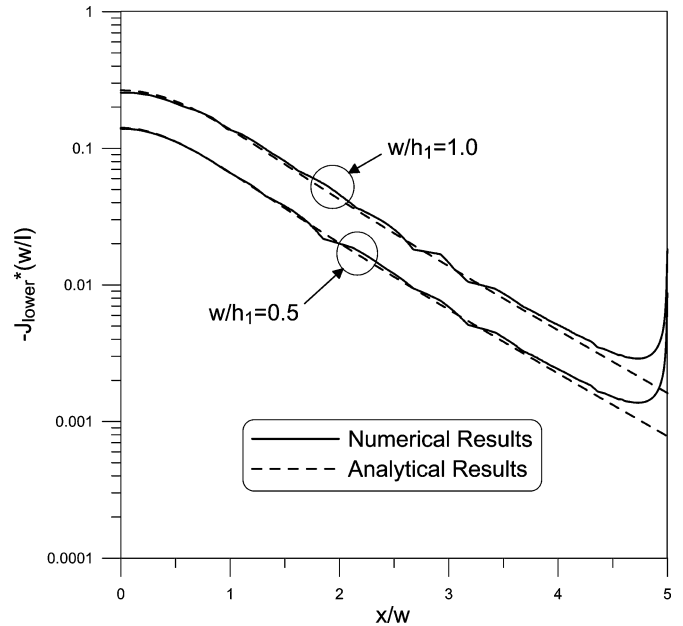


Fig. 9. Log scale comparison of analytical and numerical results for the current on the lower ground plane for $h_2 = 2h_1$.

ested in the ground plane current beyond the trace edges, and this is where the expressions presented here are most accurate for all values of w/h_1 . In any case, for most practical geometries in use today, such large values of w/h_1 are not encountered (typically $w/h_1 < 0.5$), and the analytical expressions presented here are quite accurate for all values of x/w .

Our analytical expressions were obtained by assuming that the ground planes extended to infinity. Obviously, in realistic

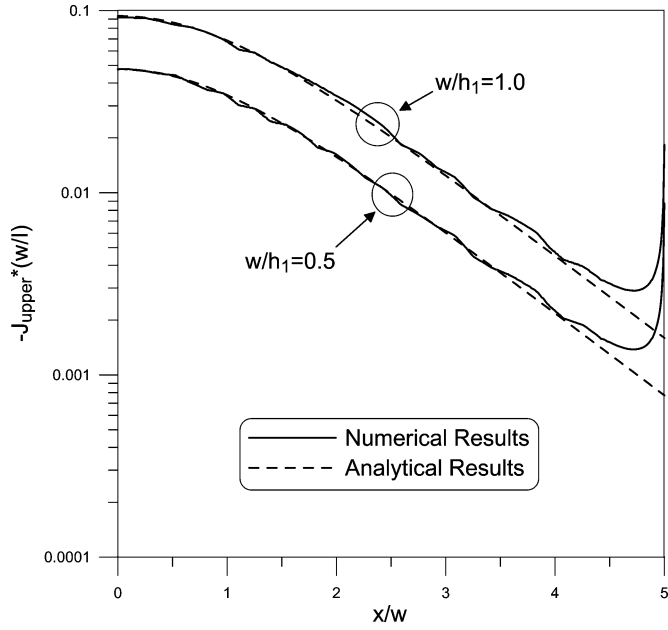


Fig. 10. Log scale comparison of analytical and numerical results for the current on the upper ground plane for $h_2 = 2h_1$.

structures, the ground planes will be large but not infinite. The numerical results for ground planes of width $10w$ allow us to illustrate the effects of a truncated ground plane. The slight increase in current density at the edges of the ground planes is shown in Figs. 8–10. Since the analytical results assume an infinite ground plane, they do not capture this effect. The increase in the current at the ground plane edges only occurs in a small region, and we see that the analytical expressions correlate quite well with the numerical results, except very near the edge. We should note that even though the current density increases at the edges, this effect contributes only a small percentage of the total current flowing on the ground planes. Obviously, the larger the ground planes are as compared to w and h_1 , the smaller the edge effects will be. It might be possible to modify the analytical results presented here in order to incorporate the edge effects. However, such a modification would be very involved and beyond the scope of this paper. This point will be the topic of future work.

VII. DEPENDENCE OF GROUND PLANE CURRENTS ON h_2/h_1

In this section, the dependence of the current distributions on h_2/h_1 is studied. If one starts with a symmetric geometry (i.e., $h_2 = h_1$) and lets h_2 increase, the current on the lower ground plane should start at the distribution of the symmetric case and approach the current distribution of a microstrip, while the current on the upper ground plane should start at the distribution of the symmetric case and go to zero. In other words, the current densities on the ground planes for an arbitrary asymmetric stripline are bounded by the current distributions of a symmetric stripline and that of a microstrip line. This is illustrated in Fig. 11 for $w/h_1 = 10$. It is interesting to observe that for $h_2 = 10h_1$, the current on the lower ground

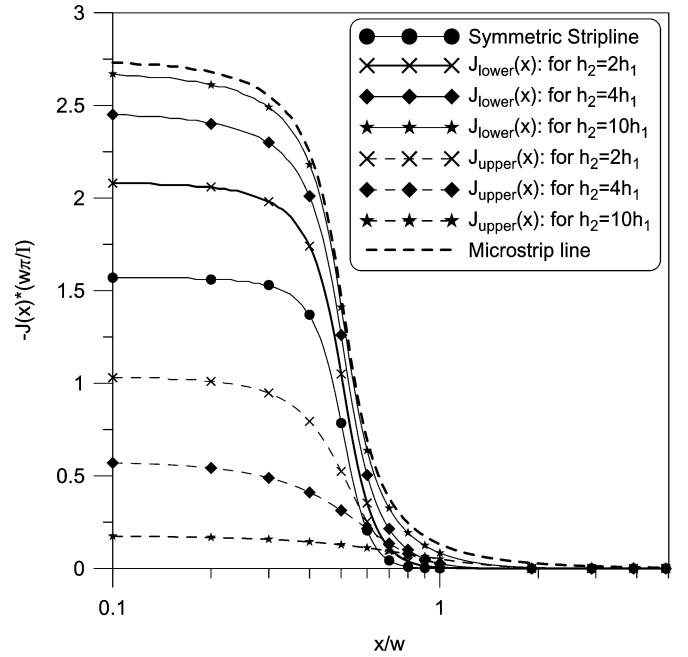


Fig. 11. Current densities of the different geometries for $w/h_1 = 10$ and various values of h_2/h_1 .

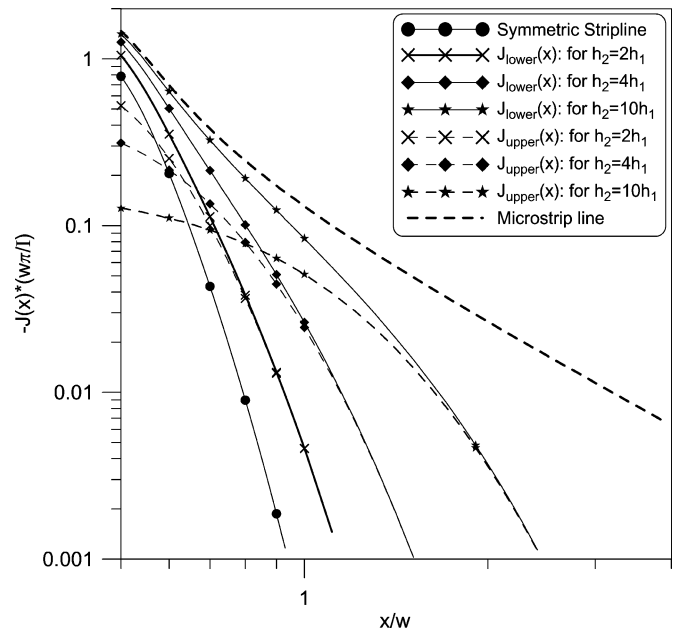


Fig. 12. Current densities of the different geometries for $w/h_1 = 10$ and various values of h_2/h_1 .

plane is well approximated by the expression for the ground plane current of the microstrip line.

The results in Fig. 11 are replotted in Fig. 12 on a log-log scale in order to emphasize the current distributions beyond the edge of the trace. Notice that for a given h_2/h_1 , the current densities on the two ground planes approach the same value as x/w gets larger. We also notice that for larger values of h_2/h_1 , the point where these two current distributions become equivalent occurs at larger values of x/w , which should be expected.

At times, it is important to know the relative amounts of total current flowing on the two ground planes. The fractional total current (normalized to the total current on the signal trace) on the lower ground plane of an asymmetric stripline is given by

$$I_{\text{lower}} = -\frac{1}{I} \int_{-\infty}^{\infty} J_{\text{lower}} dx \quad (32)$$

and the fractional total current (normalized to the total current on the signal trace) on the upper ground plane of an asymmetric stripline is given by

$$I_{\text{upper}} = -\frac{1}{I} \int_{-\infty}^{\infty} J_{\text{upper}} dx \quad (33)$$

where J_{lower} and J_{upper} are given in (24) and (23), respectively. With a little effort, these integrals can be evaluated in closed form, from which it can be shown that the percentage of the total current on the ground planes (relative to the total current on the signal trace) can be expressed as

$$\begin{aligned} I_{\text{lower}}(\%) &= \left(1 - \frac{h_1}{l}\right) \times 100 \\ I_{\text{upper}}(\%) &= \frac{h_1}{l} \times 100 \end{aligned} \quad (34)$$

Notice that I_{lower} and I_{upper} are linear with respect to h_1/l .

As expected, for $h_1/h_2 = 1.0$, 50% of the total current on the signal trace flows on each ground plane. As $h_1/l \rightarrow 0$, $I_{\text{lower}} \rightarrow 100\%$ and $I_{\text{upper}} \rightarrow 0\%$; as $h_1/l \rightarrow 1$, $I_{\text{lower}} \rightarrow 0\%$, and $I_{\text{upper}} \rightarrow 100\%$. Note that $h_1/l \rightarrow 0$ when either $h_1 \rightarrow 0$ or $l \rightarrow \infty$ (recall that $l \rightarrow \infty$ is the microstrip limit). The expressions in (34) were verified by numerically evaluating the integrals in (32) and (33), and the resulting values were indistinguishable from those obtained using the expressions in (34).

VIII. DISCUSSION AND CONCLUSION

In this paper, closed-form expressions for the current density on the ground planes of an asymmetric-stripline structure were derived. Three special cases of this stripline were studied: a symmetric stripline, a microstrip line, and a certain asymmetric stripline, where $h_2 = 2h_1$. The first two cases were used as validation of the expressions derived here, while the third occurs often in multilayer board layouts. For a symmetric-stripline geometry, the results presented here reduce to those of [6] and were derived with a different approach. If $h_2 \rightarrow \infty$, the stripline geometry becomes a microstrip line, and the results in the present paper reduce to those of [7]. It was illustrated that the current densities on the ground planes for an arbitrary asymmetric stripline are bounded by the current distributions of a symmetric stripline and of a microstrip line. For arbitrary values of h_2/h_1 , the current densities on the two different ground planes were shown to approach the same values outside the edges of the ground planes (i.e., at locations removed from under the signal trace). The analytical expressions present here were validated by comparisons to numerical results.

In this paper, we also presented expressions for the fraction of total current flowing on each of the ground planes for arbitrary

values of h_2/h_1 , where it was shown that these expressions are linear with respect to h_1/l . As expected, for $h_1/h_2 = 1.0$, 50% of the total current on the signal trace flows on each ground plane, and as h_1/h_2 (or h_1/l) becomes small, the total amount of current flowing on the lower ground plane (relative to the total current on the signal trace) approaches 100%.

The expressions derived here lend themselves to simple design procedures, whereas knowledge of these current distributions can aid in determining the amount of coupling between adjacent traces fabricated between two common ground planes, which is important for signal integrity considerations [1]–[5]. These current distributions can also aid in determining how wide-truncated ground planes need to be in order to ensure that edge effects are minimal. Knowing the current distribution can also aid in determining the loss due to the finite conductivity of the ground planes, procedures similar to those used in [6], [7], [21], and [22] can be used to determine this loss and will be the topic of future work.

ACKNOWLEDGMENT

The authors would like to thank H. Ott (of Henry Ott Consultants) and R. F. German (of German Training and Consulting), for their helpful suggestions and technical discussions, and Dr. P. Kabos (of National Institute of Standards and Technology, NIST) for helping with the finer points of [21].

REFERENCES

- [1] H. W. Johnson and M. Graham, *High-Speed Digital Design: A Handbook of Black Magic*. Englewood Cliffs, NJ: Prentice-Hall, 1993, pp. 191–192.
- [2] I. Catt, D. Walton, and M. Davidson, *Digital Hardware Design*. London, U.K.: McMillan, 1979.
- [3] E. Bogatin, *Signal Integrity Simplified*. Upper Saddle River, NJ: Prentice-Hall, 2004.
- [4] S. H. Hall, G. W. Hall, and J. A. McCall, *High Speed Digital System Design: A Handbook of Interconnect Theory and Design Practices*. New York: Wiley, 2000.
- [5] C. R. Paul, *Introduction to Electromagnetic Compatibility*. New York: Wiley, 1992.
- [6] C. L. Holloway, "Expressions for the loss of stripline and coplanar strip (CPS) structures," *Microw. Opt. Technol. Lett.*, vol. 25, pp. 162–168, 2000.
- [7] C. L. Holloway and E. F. Kuester, "Closed-form expressions for the current density on the ground plane of a microstrip line, with application to ground plane loss," *IEEE Trans. Microw. Theory Tech.*, vol. 43, no. 5, pp. 1204–1208, May 1995. Correction, *ibid.*, vol. 54, no. 11, pp. 4018–4019, Nov. 2006.
- [8] —, "Edge shape effects and quasi-closed form expressions for the conductor loss of microstrip lines," *Radio Sci.*, vol. 29, pp. 539–559, 1994.
- [9] C. L. Holloway, "Edge and surface shape effects on conductor loss associated with planar circuits," *Electromagn. Lab., Dept. Electr. Comput. Eng., Univ. Colorado, Boulder, COMIMICAD Tech. Rep. 12*, Apr. 1992.
- [10] E. F. Kuester and D. C. Chang, "Closed-form expressions for the current or charge distribution on parallel strips or microstrip," *IEEE Trans. Microw. Theory Tech.*, vol. MTT-28, pp. 254–259, 1980.
- [11] M. Kobayashi, "Longitudinal and transverse current distributions on microstriplines and their closed-form expression," *IEEE Trans. Microw. Theory Tech.*, vol. MTT-33, pp. 784–788, 1985.
- [12] W. Shumacher, "Stromverteilung auf der grundfläche der mikrostrip leitung und deren auswirkung auf die ohmsche leitungsdämpfung," *AEÜ*, band 33, pp. 207–212, 1979.
- [13] C. T. A. Johnk, *Engineering Electromagnetic Fields and Waves*. New York: Wiley, 1975, ch. 5.
- [14] B. Hague, *The Principles of Electromagnetism Applied to Electrical Machines*. New York: Dover, 1962, ch. XII.

- [15] I. S. Gradshteyn and I. M. Ryzhik, *Table of Integrals, Series and Products*. New York: Academic, 1980.
- [16] W. M. Hicks, "On velocity and electric potentials between parallel planes," *Quart. J. Pure Appl. Math.*, vol. 15, pp. 274–315, 1878.
- [17] E. W. Hobson, *A Treatise on Plane Trigonometry*, 4th ed. London, U.K.: Cambridge Univ. Press, 1918, ch. XVII.
- [18] E. T. Whittaker and G. N. Watson, *A Course of Modern Analysis*. Cambridge, U.K.: Cambridge Univ. Press, 1927, p. 137.
- [19] J. Zehentner, "Aproximace hustoty proudu symetrického třívodičového skového vedení," *Slaboproudý Obzor*, vol. 51, pp. 57–59, 1990.
- [20] D. C. Meeker. (Apr. 10, 2006 Build) *Finite Element Method Magnetics, Version 4.0.1*. [Online]. Available: <http://femm.foster-miller.net>
- [21] J. Zehentner, "Měrný útlum symetrického a nesymetrického páskového vedení," *Elektrotechnický Časopis*, vol. 40, pp. 425–436, 1989.
- [22] C. L. Holloway and G. A. Hufford, "Internal inductance associated with the ground plane of a microstrip line," *IEEE Trans. Electromagn. Compat.*, vol. 39, no. 2, pp. 73–78, May 1997.



Christopher L. Holloway (S'86–M'92–SM'04) was born in Chattanooga, TN, on March 26, 1962. He received the B.S. degree from the University of Tennessee, Chattanooga, in 1986 and the M.S. and Ph.D. degrees in electrical engineering from the University of Colorado, Boulder, in 1988 and 1992, respectively.

During 1992, he was a Research Scientist with Electro Magnetic Applications, Inc., Lakewood, CO, where he was engaged in theoretical analysis and finite-difference time-domain modeling of various electromagnetic problems. From 1992 to 1994, he was with the National Center for Atmospheric Research (NCAR), Boulder, where he was engaged in wave-propagation modeling, signal-processing studies, and radar-systems design. From 1994 to 2000, he was with the Institute for Telecommunication Sciences (ITS), U.S. Department of Commerce, Boulder. During this period, he was working on wave propagation studies. Since 2000, he has been with the National Institute of Standards and Technology (NIST), Boulder, working on electromagnetic theory. He is also a Graduate Faculty member at the University of Colorado. His current research interests include electromagnetic field theory, wave propagation, guided wave structures, remote sensing, numerical methods, and electromagnetic compatibility/electromagnetic interference (EMC/EMI) issues. He is an Associate Editor of the IEEE TRANSACTIONS ON ELECTROMAGNETIC COMPATIBILITY.

Dr. Holloway was awarded the 2006 Department of Commerce Bronze medal for his work in radio wave propagation, the 1999 Department of Commerce Silver Medal for his work in electromagnetic theory, and the 1998 Department of Commerce Bronze Medal for his work on printed circuit boards. He is a member of Commission A of the International Union of Radio Science. During 2000–2005, he was Chairman for the Technical Committee on Computational Electromagnetics (TC-9) of the IEEE Electromagnetic Compatibility Society and is currently serving as an IEEE Distinguished Lecturer for the EMC Society.



Edward F. Kuester (S'73–M'76–SM'95–F'98) received the B.S. degree from Michigan State University, East Lansing, in 1971 and the M.S. and Ph.D. degrees from the University of Colorado, Boulder, in 1974 and 1976, respectively, all in electrical engineering.

Since 1976, he has been with the Department of Electrical and Computer Engineering, University of Colorado, where he is currently a Professor. In 1979, he was a Summer Faculty Fellow at the Jet Propulsion Laboratory, Pasadena, CA. During 1981–1982,

he was a Visiting Professor at the Technische Hogeschool, Delft, The Netherlands. During 1992–1993, he was Professeur Invité at the École Polytechnique Fédérale de Lausanne, Switzerland. He was a Visiting Scientist at the National Institute of Standards and Technology (NIST), Boulder, in 2002, 2004, and 2006. His current research interests include the modeling of electromagnetic phenomena of guiding and radiating structures, applied mathematics, and applied physics. He is the coauthor of one book, the author of chapters in two others, and translator of two Russian books. He is coholder of two U.S. patents and author or coauthor of more than 60 papers in refereed technical journals and numerous conference presentations.

Dr. Kuester is a Fellow of the IEEE Antennas and Propagation (AP), IEEE Microwave Theory and Techniques (MTT), and IEEE Electromagnetic Compatibility (EMC) Societies, a member of the Society for Industrial and Applied Mathematics, and a member of Commissions B and D of the International Union of Radio Science.